PHYSICAL REVIEW D **81,** 035009 (2010)

# Predictions for $m_t$ and $M_W$ in minimal supersymmetric models

O. Buchmueller,[1] R. Cavanaugh,[2,3] A. De Roeck,[4,5] J. R. Ellis,[4] H. Flächer,[6] S. Heinemeyer,[7] G. Isidori,[8,9]
Keith A. Olive,[10] F. J. Ronga,[11] and G. Weiglein[12]

[1]*High Energy Physics Group, Imperial College, Blackett Laboratory, Prince Consort Road, London SW7 2AZ, United Kingdom*
[2]*Fermi National Accelerator Laboratory, P.O. Box 500, Batavia, Illinois 60510, USA*
[3]*Physics Department, University of Illinois at Chicago, Chicago, Illinois 60607-7059, USA*
[4]*CERN, CH–1211 Genève 23, Switzerland*
[5]*Antwerp University, B–2610 Wilrijk, Belgium*
[6]*Department of Physics and Astronomy, University of Rochester, Rochester, New York 14627, USA*
[7]*Instituto de Física de Cantabria (CSIC-UC), E–39005 Santander, Spain*
[8]*INFN, Laboratori Nazionali di Frascati, Via E. Fermi 40, I–00044 Frascati, Italy*
[9]*Institute for Advanced Study, Technische Universität München, Arcisstraße 21, D-80333 München, Germany*
[10]*William I. Fine Theoretical Physics Institute, University of Minnesota, 116 Church Street SE, Minneapolis, Minnesota 55455, USA*
[11]*Institute for Particle Physics, ETH Zürich, CH–8093 Zürich, Switzerland*
[12]*DESY, Notkestrasse 85, D–22603 Hamburg, Germany*

(Received 8 December 2009; published 11 February 2010)

Using a frequentist analysis of experimental constraints within two versions of the minimal supersymmetric extension of the standard model, we derive the predictions for the top quark mass, $m_t$, and the $W$ boson mass, $M_W$. We find that the supersymmetric predictions for both $m_t$ and $M_W$, obtained by incorporating all the relevant experimental information and state-of-the-art theoretical predictions, are highly compatible with the experimental values with small remaining uncertainties, yielding an improvement compared to the case of the standard model.

DOI: 10.1103/PhysRevD.81.035009 PACS numbers: 12.60.Jv, 14.65.Ha, 14.70.Fm

One of the most impressive successes of the standard model (SM) has been the accurate prediction of the mass of the top quark obtained from a fit to precision electroweak measurements at LEP and the SLC [1], which agrees very well with the value measured at the Tevatron [2]. To this may be added the equally successful prediction of the $W$ mass [1,3]. The successes of these comparisons between theory and experiment require the incorporation of higher-order quantum corrections. In the SM, these receive contributions from the postulated Higgs boson. Indeed, the precision data favor a relatively light Higgs boson weighing $\lesssim 150$ GeV [1].

One theoretical framework that predicts such a light Higgs boson is supersymmetry (SUSY) [4], which also possesses the ability to render more natural the electroweak mass hierarchy, contains a plausible candidate for astrophysical dark matter, facilitates grand unification, and offers a possible explanation of the apparent discrepancy between the experimental measurement of the anomalous magnetic moment of the muon, $(g-2)_\mu$, and the theoretical value calculated within the SM. There have been many analyses of the possible masses of particles within the minimal supersymmetric (MSSM) extension of the standard model, taking into account the experimental, phenomenological, and astrophysical constraints. For example, we have presented sparticle mass predictions [5–7] on the basis of a frequentist analyses of the relevant constraints in the context of simple models for SUSY breaking such as the constrained minimal supersymmetric standard model (CMSSM) (in which the input scalar masses $m_0$, gaugino masses $m_{1/2}$ and soft trilinear parameters $A_0$ are each universal at the grand unified theory scale) and the model with one nonuniversal Higgs mass (NUHM1) (in which a common SUSY-breaking contribution to the Higgs masses is allowed to be nonuniversal). For an extensive list of references, see [7].

These analyses favor relatively light masses for the sparticles, indicating significant sensitivity of the precision observables to quantum effects of supersymmetric particles. It is therefore desirable to revisit the successful predictions of the SM, in particular, the show-case predictions of $m_t$ and $M_W$, to see how they are affected in the CMSSM and NUHM1. In particular, one may ask whether the SM prediction of $m_t$ and $M_W$ is improved, relaxed or otherwise altered in these models. The answer to this key question is highly nontrivial, since low-mass sparticles such as the $\tilde{t}$ and $\tilde{b}$ may contribute significantly to the prediction of electroweak observables [8], and the (lightest) Higgs mass is no longer an independent quantity, but also depends on the sparticle masses as we discuss below.

In this article, for the first time, we make supersymmetric predictions for $m_t$ and $M_W$, as have been performed so far only within the SM [1]. Here, we work within the same framework as in our previous frequentist analyses of the CMSSM and NUHM1 parameter spaces [5–7]. The treatments of the experimental, phenomenological and astrophysical constraints are nearly identical with those in [7]. Here, we employ the updated SM value of $(g-2)_\mu$ which includes a new set of low-energy $e^+e^-$ data [9]. The new value of $(g-2)_\mu$ [10] does not significantly alter the regions of the CMSSM and NUHM1 parameter spaces favored in our previous analyses.

Our statistical treatment of the CMSSM and NUHM1 makes use of a large sample of points (about $3 \times 10^6$) in the SUSY parameter spaces obtained with the Markov Chain Monte Carlo technique. Our analysis is entirely frequentist. This enables us to avoid any ambiguity associated with the choices of Bayesian priors. Indeed, within the Bayesian approach, it has been shown that results for the best-fit regions of the CMSSM parameter space obtained from current data (i.e. electroweak precision data, etc.) are very sensitive to the choice of priors [11], but this would no longer be the case in a situation where plenty of LHC results were available. The evaluations are performed using the `MasterCode` [5–7,12], which includes the following theoretical codes. For the renormalization group equation running of the soft SUSY-breaking parameters, it uses `SoftSUSY` [13], which is combined consistently with the codes used for the various low-energy observables: `FeynHiggs` [14–16] is used for the evaluation of the Higgs masses and $a_\mu^{\rm SUSY}$ (see also [8,17]), for the other electroweak precision data we have included a code based on [18,19], `SuFla` [20,21] and `SuperIso` [22,23] are used for flavor-related observables, and for dark-matter-related observables `MicrOMEGAs` [24] and `DarkSUSY` [25] are used. In the combination of the various codes, `MasterCode` makes extensive use of the SUSY Les Houches Accord [26,27].

In the SM, the precision of the confrontation between theory and experiment is often expressed in the $(m_t, M_W)$ plane. The experimental values of these quantities are essentially uncorrelated [1–3],

$$m_t^{\rm exp} = 173.1 \pm 1.3\ {\rm GeV}, \tag{1}$$

$$M_W^{\rm exp} = 80.399 \pm 0.023\ {\rm GeV}, \tag{2}$$

shown in Fig. 1 as the black ellipse. In the SM, $m_t$ is an independent input parameter; whereas, the relation between the gauge boson masses $M_W$ and $M_Z$ can be predicted with high precision in terms of $m_t$, the Higgs mass, $M_H^{\rm SM}$, and other model parameters; see [28], and references therein. The correlation between $m_t$ and the prediction for $M_W$ is displayed in Fig. 1 (foliated by lines of constant Higgs mass, $M_H^{\rm SM}$).

A fit of the SM parameters to precision observables, e.g., those measured at the $Z$ peak [29], yields indirect predictions for $m_t$ and $M_H^{\rm SM}$, and hence also a prediction for $M_W$. The SM prediction for $m_t$ without including the experimental limits on $M_H^{\rm SM}$ and excluding or including the experimental measurement of $M_W$ is [1]

$$m_t^{{\rm fit,SM,excl.}M_W} = 172.6^{+13.3}_{-10.2}\ {\rm GeV}, \tag{3}$$

$$m_t^{{\rm fit,SM,incl.}M_W} = 179.3^{+11.6}_{-8.5}\ {\rm GeV}, \tag{4}$$

and the SM prediction for $M_W$, excluding the experimental measurement of $M_W$ but either excluding or including the experimental measurement of $m_t$ is [1]

$$M_W^{{\rm fit,SM,excl.}m_t} = 80.363 \pm 0.032\ {\rm GeV}, \tag{5}$$

$$M_W^{{\rm fit,SM,incl.}m_t} = 80.364 \pm 0.020\ {\rm GeV}. \tag{6}$$

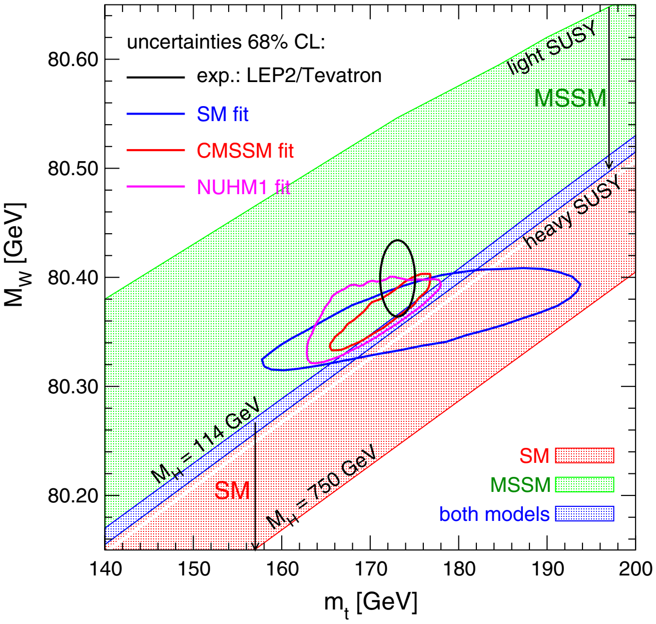

FIG. 1 (color online). The 68% C.L. regions in the $(m_t, M_W)$ plane predicted by a SM fit excluding the LEP Higgs constraint [1], and by CMSSM and NUHM1 fits including the LEP Higgs mass constraint, compared with the experimental measurements from LEP2 and the Tevatron shown as the black ellipse. The medium gray (red) and the dark (blue) shaded regions show the SM prediction, foliated by lines of constant $M_H^{\rm SM}$ values. The light gray (green) and the dark (blue) regions show the prediction of the unconstrained MSSM [18] ranging from light to heavy SUSY particles.

The regions of the $(m_t, M_W)$ plane favored at the 68% C.L. by direct experimental measurements (1) and (2) and in the SM fit (3) and (5), shown as the dark (blue) contour [30] in Fig. 1 have significant overlap, representing a nontrivial success for the SM at the quantum level. However, we note that the overlap between the 68% C.L. contours happens in the region of Higgs mass values that are below the exclusion bound from the LEP SM Higgs searches, $M_H^{\rm SM} > 114.4$ GeV [31], indicating a certain tension between the precision observables and the Higgs limit. Indeed, the experimental central value of $M_W$ would be reached for a Higgs mass as low as $M_H^{\rm SM} \sim 60$ GeV. Combining the indirect measurements, $m_t$ and $M_W$, the best-fit value of $M_H^{\rm SM} \sim 87$ GeV, and the 95% C.L. upper limit is $M_H^{\rm SM} \sim 157$ GeV [1]. The direct searches at the Tevatron currently exclude a range 163 GeV $< M_H^{\rm SM} <$ 166 GeV [32], as also indicated by a white line in Fig. 1, so that the range 115 GeV $\lesssim M_H^{\rm SM} \lesssim$ 150 GeV is favored in a global fit to the SM (including experimental bounds) at the 95% C.L. [33].

Turning now to our analysis in the case of supersymmetry, we note that the prediction for $M_W$ as a function of $m_t$ in the unconstrained MSSM gives rise to a band in Fig. 1 (shaded green) which has only little overlap (shaded blue) with the band showing the range of SM predictions for Higgs masses above the search limit from LEP. This is because the contribution of light supersymmetric particles tends to increase the predicted value of $M_W$ compared to the SM case. Furthermore, the overlap region (corresponding to the situation where all supersymmetric particles are heavy) is limited because, in contrast to the SM, the value of $M_h$ is not an independent parameter in the MSSM, but is calculable in terms of the sparticle masses with an upper limit ~135 GeV [15].

We have performed fits in the CMSSM and the NUHM1 including all relevant experimental information as specified in [7], i.e., we include all precision observables used in the SM fit shown in Fig. 1 (except $\Gamma_W$, which has a minor impact) as well as constraints from $(g-2)_\mu$, flavor physics, the cold dark matter relic density and the direct searches for the Higgs boson and supersymmetric particles. The direct experimental measurements of $M_W$ and $m_t$, on the other hand, have *not* been included in these global fits. The results of our fits in the CMSSM and the NUHM1 are also displayed as 68% C.L. contours in Fig. 1 and show remarkably good agreement with the experimental measurements of $M_W$ and $m_t$.

The 68 and 95% C.L. regions in the $(m_t, M_W)$ plane found in the CMSSM (NUHM1) fit are shown in more detail in the left (right) panel of Fig. 2. The fits within the MSSM differ from the SM fit in various ways. First, the number of free parameters is substantially larger in the MSSM, even restricting ourselves to the CMSSM and the NUHM1. On the other hand, more observables are included in the fits, providing extra constraints. We recall that in the SM fits $(g-2)_\mu$ and the $B$-physics observables have a minor impact on the best-fit regions, and are not included in the results shown above, which are taken from [1] (see e.g. [34] for an alternative approach), while the relic density of cold dark matter cannot be accommodated in the SM. Furthermore, as already noted, whereas the light Higgs boson mass is a free parameter in the SM, it is a function of the other parameters in the CMSSM and NUHM1. In this way, for example, the masses of the scalar tops and bottoms enter not only directly into the prediction of the various observables, but also indirectly via their impact on $M_h$. This provides additional motivation for including the experimental constraints on $M_h$ into the fits in the MSSM.

In Fig. 3, we show the results of the same fit as in Fig. 2, but now in the $(M_h, m_t)$ plane for the CMSSM (NUHM1) in the left (right) panel. The LEP lower limit of 114 GeV is applicable in the CMSSM [35,36], but cannot always be directly applied in the NUHM1, since there are regions of the NUHM1 parameter space where the $hZZ$ coupling is suppressed relative to its value in the SM [37]. We use the

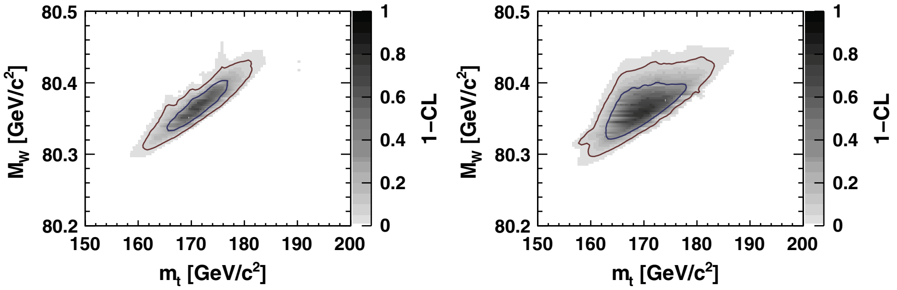

FIG. 2 (color online). The 68% and 95% C.L. regions in the $(m_t, M_W)$ planes for the CMSSM (left) and for the NUHM1 (right), for fits that do not include the direct measurements of $m_t$ and $M_W$, but do incorporate the appropriate LEP constraint on $M_h$.

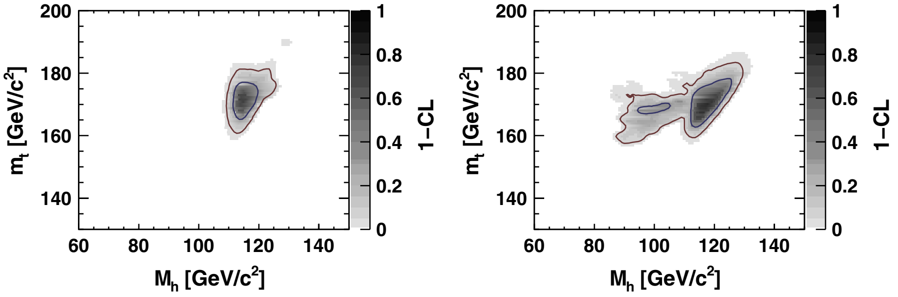

FIG. 3 (color online). The 68% and 95% C.L. regions in the $(M_h, m_t)$ planes for the CMSSM (left plot) and for the NUHM1 (right plot), for fits that do not include the direct measurements of $m_t$ and $M_W$, but do incorporate the appropriate LEP constraint on $M_h$.

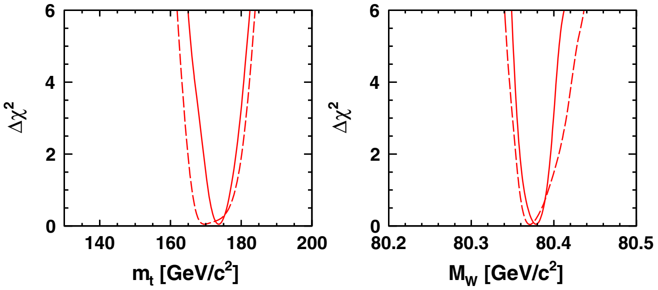

FIG. 4 (color online). The $\chi 2$ functions for $m_t$ (left panel) in the CMSSM (solid) and NUHM1 (dashed) excluding the direct $m_t$ mass measurement but including all the other experimental information. The corresponding $\chi 2$ functions for $M_W$ (right panel) excluding the direct $M_W$ mass measurement but again including all the other experimental information.

prescription given in [7] to calculate the $\chi^2(M_h)$ contribution for points with suppressed $hZZ$ couplings, and see in the right panel of Fig. 3 a significant set of NUHM1 points with $M_h \ll 114$ GeV: these reflect the shape of the $\Delta\chi^2$ function in the right panel of Fig. 4 of [7].

We now turn to the single-variable $\chi^2$ functions for $m_t$ and $M_W$. In the left panel of Fig. 4, we show the $\chi^2$ functions for $m_t$ in the CMSSM and NUHM1 as solid and dashed lines, respectively, with $M_W$ included in the fit (as before, the direct measurement of $m_t$ is not included in this fit). Comparing the results with the SM fit, we find that these rise more sharply, in particular, for larger values of $m_t$, than they would in the SM fit, indicating that the upper bound on $m_t$ from the indirect prediction in the MSSM is significantly reduced compared to the SM case. We find the 68% C.L. ranges

$$m_t^{\mathrm{fit,CMSSM,incl.}M_W} = 173.8^{+3.2}_{-3.1}\ \mathrm{GeV}, \tag{7}$$

$$m_t^{\mathrm{fit,NUHM1,incl.}M_W} = 169.5^{+8.8}_{-3.4}\ \mathrm{GeV}. \tag{8}$$

Comparing with the SM fit result (4), we find lower central values for $m_t$ in both the CMSSM and NUHM1 in better agreement with the experimental result (1). The reduction in the upper bound on $m_t$ reflects, in particular, the fact that the additional contribution from the $\tilde{t}$ and $\tilde{b}$ enters with the same sign as the leading SM-type contribution to the precision observables that is proportional to $m_t^2$. A nonvanishing contribution from superpartners therefore tends to reduce the preferred value of $m_t$ compared to the SM fit. It should be noted in this context that the smaller uncertainties in $m_t$ found in the supersymmetric fits compared to the SM case (particularly in the CMSSM) can in part also be attributed to the fact that a larger set of observables has been used in the CMSSM and NUHM1 fits.

For the $W$ boson mass, we find the $\chi^2$ functions including $m_t$ in the fit in the CMSSM (solid) and NUHM1 (dahed) shown in the right panel of Fig. 4, and the corresponding 68% C.L. ranges

$$M_W^{\mathrm{fit,CMSSM,incl.}m_t} = 80.379^{+0.013}_{-0.014}\ \mathrm{GeV}, \tag{9}$$

$$M_W^{\mathrm{fit,NUHM1,incl.}m_t} = 80.370^{+0.024}_{-0.011}\ \mathrm{GeV}. \tag{10}$$

The best-fit values of these predictions are substantially higher than the SM prediction (6) based on precision electroweak data (in particular in the CMSSM) and are closer to the experimental value (2), again with smaller uncertainties.

We summarize our main results in Fig. 5. The left (right) panel compares the experimental measurement of $m_t$ ($M_W$) with the predictions of a SM fit to precision electroweak data and our final predictions in the CMSSM and NUHM1. *The resulting agreement of the final predictions for* $m_t$ *with*

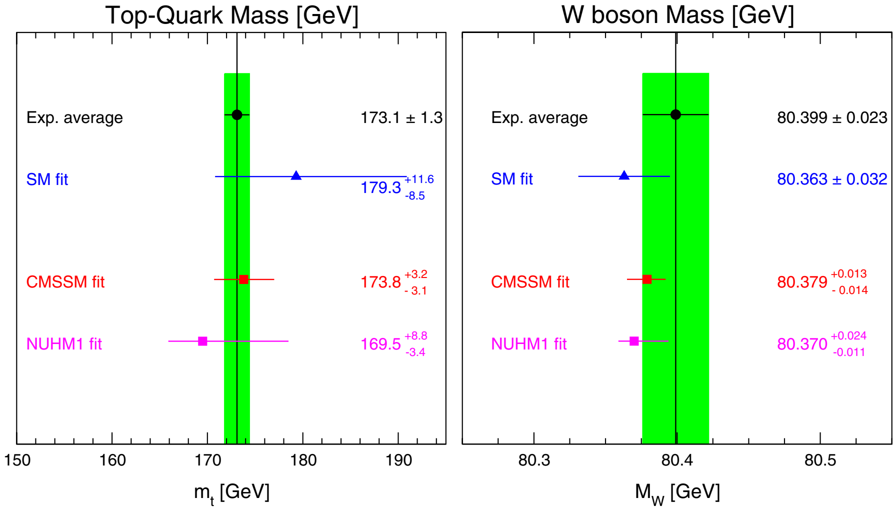

FIG. 5 (color online). The 68% C.L. ranges for $m_t$ (left panel) and $M_W$ (right panel) including (from top to bottom) the experimental average, and the predictions of the SM (not incl. the $M_H^{\mathrm{SM}}$ limits) [1], CMSSM and NUHM1 fits, using all the available information except the direct mass measurement.

*the experimental value* (1) *is remarkable, almost embarrassingly good in the CMSSM case* and very good in the NUHM1. Compared to the SM fit, the best-fit values for $M_W$ in the CMSSM and NUHM1 are closer to the experimental value (2), and in the CMSSM case the best-fit value lies within the experimental 68% C.L. range. We conclude that the CMSSM and NUHM1 pass with flying colors the test of reproducing the successful SM predictions of $m_t$ and $M_W$, even improving on them. We can only hope that this probe of SUSY at the loop level will soon be made even more precise with the discovery of sparticles at the LHC.

This work was supported in part by the European Community's Marie-Curie Research Training Network under Contracts No. MRTN-CT-2006-035505 ''Tools and Precision Calculations for Physics Discoveries at Colliders'' and No. MRTN-CT-2006-035482 ''FLAVIAnet'', and by the Spanish MEC and FEDER under Grant No. FPA2005-01678. The work of S. H. was supported in part by CICYT (Grant No. FPA 2007–66387), and the work of K. A. O. was supported in part by DOE Grant No. DE–FG02–94ER–40823 at the University of Minnesota.

---

[1] LEP Electroweak Working Group, http://lepewwg.web.cern.ch.
[2] Tevatron Electroweak Working Group, CDF Collaboration, and D0 Collaboration, arXiv:0903.2503.
[3] Tevatron Electroweak Working Group, arXiv:0908.1374.
[4] H. E. Haber and G. L. Kane, Phys. Rep. **117**, 75 (1985).
[5] O. Buchmueller *et al.*, Phys. Lett. B **657**, 87 (2007).
[6] O. Buchmueller *et al.*, J. High Energy Phys. 09 (2008) 117.
[7] O. Buchmueller *et al.*, Eur. Phys. J. C **64**, 391 (2009).
[8] S. Heinemeyer, W. Hollik, and G. Weiglein, Phys. Rep. **425**, 265 (2006).
[9] B. Aubert *et al.* (*BABAR* Collaboration), Phys. Rev. Lett. **103**, 231801 (2009).
[10] M. Davier, A. Hoecker, B. Malaescu, C. Z. Yuan, and Z. Zhang, arXiv:0908.4300.
[11] B. C. Allanach, K. Cranmer, C. G. Lester, and A. M. Weber, J. High Energy Phys. 08 (2007) 023.
[12] See http://cern.ch/mastercode.
[13] B. C. Allanach, Comput. Phys. Commun. **143**, 305 (2002).
[14] S. Heinemeyer, W. Hollik, and G. Weiglein, Comput. Phys. Commun. **124**, 76 (2000); Eur. Phys. J. C **9**, 343 (1999); see http://www.feynhiggs.de.
[15] G. Degrassi *et al.*, Eur. Phys. J. C **28**, 133 (2003).
[16] M. Frank *et al.*, J. High Energy Phys. 02 (2007) 047.
[17] T. Moroi, Phys. Rev. D **53**, 6565 (1996); **56**, 4424(E) (1997).
[18] S. Heinemeyer *et al.*, J. High Energy Phys. 08 (2006) 052.
[19] S. Heinemeyer, W. Hollik, A. M. Weber, and G. Weiglein, J. High Energy Phys. 04 (2008) 039.
[20] G. Isidori and P. Paradisi, Phys. Lett. B **639**, 499 (2006).
[21] G. Isidori, F. Mescia, P. Paradisi, and D. Temes, Phys. Rev. D **75**, 115019 (2007), and references therein.
[22] F. Mahmoudi, Comput. Phys. Commun. **178**, 745 (2008); **180**, 1579 (2009).
[23] D. Eriksson, F. Mahmoudi, and O. Stal, J. High Energy Phys. 11 (2008) 035.
[24] G. Belanger, F. Boudjema, A. Pukhov, and A. Semenov, Comput. Phys. Commun. **176**, 367 (2007); **149**, 103 (2002); **174**, 577 (2006).
[25] P. Gondolo *et al.*, New Astron. Rev. **49**, 149 (2005); J. Cosmol. Astropart. Phys. 07 (2004) 008.
[26] P. Skands *et al.*, J. High Energy Phys. 07 (2004) 036.
[27] B. Allanach *et al.*, Comput. Phys. Commun. **180**, 8 (2009).
[28] M. Awramik, M. Czakon, A. Freitas, and G. Weiglein, Phys. Rev. D **69**, 053006 (2004).
[29] ALEPH Collaboration, DELPHI Collaboration, L3 Collaboration, OPAL Collaboration, SLD Collaboration, LEP Electroweak Working Group, SLD Electroweak Group, and SLD Heavy Flavour Group, Phys. Rep. **427**, 257 (2006).
[30] http://lepewwg.web.cern.ch/LEPEWWG/plots/summer2009/s09_mt_mw_contours.eps.
[31] R. Barate *et al.* (ALEPH, DELPHI, L3, OPAL Collaborations, and LEP Working Group), Phys. Lett. B **565**, 61 (2003).
[32] CDF Collaboration and D0 Collaboration, arXiv:0911.3930.
[33] H. Flacher *et al.*, Eur. Phys. J. C **60**, 543 (2009); see http://www.cern.ch/gfitter.
[34] C. Amsler *et al.* (Particle Data Group), Phys. Lett. B **667**, 1 (2008).
[35] J. R. Ellis, S. Heinemeyer, K. A. Olive, and G. Weiglein, Phys. Lett. B **515**, 348 (2001).
[36] S. Ambrosanio *et al.*, Nucl. Phys. **B624**, 3 (2002).
[37] S. Schael *et al.* (ALEPH, DELPHI, L3, OPAL Collaborations, and LEP Working Group), Eur. Phys. J. C **47**, 547 (2006).